# DEVELOPMENT OF A COMPUTATIONAL MODEL TO DETERMINE PERFORMANCE OF A SELF-PRIMING VENTURI SCRUBBER FOR THORIUM REACTOR

**Paridhi Goel[a],*, Avinash Moharana[b] and A.K Nayak[a,b]**

**[a]Homi Bhabha National Institute, Anushaktinagar, Mumbai – 400094, India**
**Email: paridhi.hbtibe@gmail.com**
**[b]Reactor Engineering Division, Bhabha Atomic Research Centre,Trombay, Mumbai–400085, India**

## ABSTRACT

Following the post-Fukushima measures on reactor safety, the Filtered Containment Venting System (FCVS) is a mandatory to all Nuclear Power Plants worldwide. In order to ensure the capture and retention of the released radioactive fission products, the FCVS employs a manifold of self-priming venturi scrubbers submerged in a pool of liquid. The performance of the venturi scrubber significantly affects the overall performance of the system. To arrive at an efficient venturi design, a computational model is proposed to evaluate the pressure drop and the capture efficiency of the scrubber. The gas phase is modeled using an Eulerian approach while the dispersed droplets and the aerosol particulates are tracked through a Lagrangian approach. The model includes atomization of liquid jet, breakup of droplets and interaction of gas and liquid droplets. The collision efficiency of the scrubber is based on single droplet capture efficiency with the assumption that capture occurs only if the aerosol particulates and the droplets exist in the same computational cell. The numerical results show a qualitative match with earlier experimental data for pressure drop and collection efficiency.

**KEYWORDS:** FCVS , Eulerian-Lagrangian, pressure drop, collection efficiency

## 1. INTRODUCTION

In the event of severe accident at Nuclear Power Plants, the containment pressure may rise beyond the design pressure limit of the containment which may compromise the structural integrity of the containment. The Filtered Containment Venting System (FCVS) is designed to depressurize the containment and to limit the radioactive release to the atmosphere. The FCVS chiefly comprises of a scrubber tank accommodating circumferentially distributed venturi manifold and a metallic filter fiber. Venturi scrubber is one of the most important components of this passive system. It mainly comprises of three segments: converging section which accelerates the gas and particulate aerosols, throat section wherein liquid droplets introduced through orifices and aerosols drifting with gas interact and diffuser section which accounts for the pressure recovery and decrease in gas velocities. The droplets capture the aerosols mainly by inertial impaction (Boll et al. 1973). The working of venturi scrubber is hence highly dependent on the interaction of three phases comprising of particulates, liquid droplets and continuous gas stream. The performance of scrubber is measured in terms of the pressure drop and the overall collection efficiency. Researchers in the past have relied on a set of empirical co-relations to predict the pressure drop, the droplet diameter for a given scrubber dimension. The prediction of collection efficiency is based on these empirical relations, hence results in a limited range of applicability.

Pak and Chang (2006) numerically predicted pressure drop and collection efficiency of Haller et al. (1989) geometry using an Eulerian frame for gas phase and Lagrangian frame for aerosol and droplets. The results were in agreement with experimental data for pressure drop in the converging section and throat but under predicted pressure recovery in the diverging section. Similar numerical studies on the same geometry were conducted by Goniva et al. (2009) using Open FOAM. The results for simulated pressure drop were in good agreement with experimental data but the predicted collection efficiency was not satisfying for higher gas flow rates. Majid Ali et al. (2013) simulated venturi scrubber performance using Ansys CFX and validated the methodology with their experimental results. Their simulations results concurred well with experimental values at low gas velocities but gave qualitative trend for efficiency calculation at high gas velocities. Sharifi et al. (2012) conducted numerical studies to calculate pressure drop using Eulerian-Eulerian two fluid models and MUSIG model for droplet distribution and validated the model with Vishwanathan et al. (1998) results. They further investigated effect of nozzle diameter and nozzle arrangement on the pressure drop. Their results revealed that the pressure drop is unaffected by variation of nozzle diameter and their arrangements within the venturi for identical operating conditions. Numerical studies by Guerra et al. (2012) implemented Eulerian-Eulerian technique for identifying the distribution of liquid in the throat section at varying gas velocities and liquid flow rates concluding that jet penetration is a function of number of orifices and their arrangement at a constant liquid flow rate.

In this paper, a computational model is developed to predict the pressure drop and collection efficiency for a self-priming type venturi scrubber. The results obtained are validated with published experimental data (Haller et. al. (1989)). The flow was numerically solved by using an Eulerian-Lagrangian approach wherein the gas phase was treated in continuum and the dispersed phase was tracked throughout the flow domain. The model includes atomization of liquid jet, breakup of droplets and interaction of gas and liquid droplets. The collision efficiency of the scrubber is based on single droplet capture efficiency with the assumption that capture occurs only if the aerosol particulates and the droplets exist in the same computational cell. The numerical results show qualitative match with earlier experimental data for pressure drop.

## 2.  MODEL DESCRIPTION

### 2.1 Eulerian Gas Flow

For the gas phase flow an Eulerian approach is employed and the flow equation is solved using Reynolds Averaged Navier Stokes Equation with RNG k-ε turbulence model. Since the loading ratio of aerosols is very low (~$O(10^{-6})$) one way coupled flow conditions can be considered. Also the heat transfer between the gas flow and particulates is neglected maintaining isothermal conditions. The flow is incompressible and discrete phase is kept inert thus neglecting chemical interaction and mass transfer.

### 2.2 Lagrangian Tracking of Droplets and Aerosols

The motion of droplets and aerosols is followed using Lagrangian frame where discrete particles are tracked. Their momentum equation is described by simplified Basset-Boussinesq-Oseen equation (B-B-O). To reduce the computational complexity particles having identical diameter, velocity and spatial position are clubbed and referred as parcel. The properties of parcels are therefore updated after each particle simulation. Since density of particles is higher compared to continuum gas virtual mass, Basset force can be neglected. The gravity force is also neglected considering that aerodynamic forces govern the

flow field. Amongst these, the drag force dominates the flow dynamics of the dispersed phase; hence for the present analysis coupling between the phases is achieved through the drag term alone.

## 2.3 Droplet Deformation and drag

The drag coefficient for the particles is approximated by dynamic drag model incorporating droplet distortion. The correlation is expressed as

$$C_{D,sphere} = 0.424 \quad Re > 1000$$

$$C_{D,sphere} = \frac{24}{Re}(1 + \frac{1}{6}Re^{0.67}) \quad Re < 1000$$

$$C_D = C_{D,sphere}(1 + 2.63y)$$

where y accounts for the distortion of droplet (y=0 implies spherical particle and y=1 corresponds to a disk) and is calculated from TAB model.

## 2.4 Atomization and break up of jet stream

After injection from throat orifices the liquid jet stream disintegrates into thin lamella to undergo secondary break up forming droplets. The formation of droplets occurs within few millimeters depending on relative velocity of injected stream and incoming gas stream (Mayinger et al. 1978). The two governing forces governing the break up are surface tension and aerodynamic drag. The liquid jet inserted in the high convective stream emerges as a column. The column then subjected to aerodynamic drag starts bending in the direction of flow counter balancing the accelerative forces to a certain point known as column break-up.

Modeling of this is approached using Reitz wave instability model where the break-up column time is determined from Wu et al. (1997). The instabilities observed on the cross-injection of liquid stream in convective high speed gas stream causes ripples and disturbances on the surface of liquid jet. The droplet breakup is proportional to the growth of the fastest growing instability.

$$t_{cb} = 5\frac{d}{u_{gth}}\sqrt{\frac{\rho_d}{\rho}}$$

## 2.5 Capture of aerosol

Collection of aerosol particles is due to the collision of the droplets with aerosols. There are various collection mechanisms viz. inertial impaction, diffusion, interception described in literature depending on the dimension of the discrete particle. As pointed out by Boll et al. (1973) inertial impaction is observed to be the dominating mechanism in Venturi scrubbers for capturing micron sized particles. Inertial impaction ($\eta$) is a function of Stokes number ($K_p$) as given in equation where $K_p$ is the ratio of the particle (aerosol) stopping distance to the radius of the collector (droplet). The Stokes number characterizes interaction of particulates with flow field. For potential flow and for values $K_p$ greater than 0.2, single drop inertial collection efficiency is approximated by Calvert et al.(1970):

$$K_p = \frac{d_p^2 (\boldsymbol{u}_s - \boldsymbol{u}_d)^2}{9\,\mu_g d_d}$$

$$\eta = \left(\frac{K_p}{K_p + 0.7}\right)^2$$

Capture of aerosol is modeled with the prime assumption that capture occurs only when the aerosol and droplets occupy the same computational cell. Assuming uniform distribution of X aerosols parcels having $N_s$ number of aerosols in it and Y droplet parcels having $N_d$ number of droplets in a computational cell then the collection efficiency of one droplet parcel is computed by given equation

$$N_{cap} = \eta \frac{\pi}{4} d_d^2 |\boldsymbol{u}_s - \boldsymbol{u}_d| \frac{N_d . N_s . \tau}{dV}$$

The collection efficiency of the computational cell is given by the summation of individual parcel interactions in that cell.

$$N_{cell} = \sum_{m=1}^{M} \sum_{n=1}^{N} N_{cap}$$

## 3. NUMERICAL METHODOLOGY

The 3D hybrid mesh of a venturi scrubber is discretized into 154,147 cells and 85,243 nodes as shown in Fig1. The computational domain includes entry and exit ducts to avoid unreal turbulence in the flow. The converging and diverging sections of mesh are discretized into hexahedral cells while at the throat hybrid hex core mesh with tetrahedral layer at the outer is constructed. The convergence criteria for all variables is set to $10^{-3}$ and second order upwind scheme was set for discretization of momentum equations and first order for turbulent parameters.
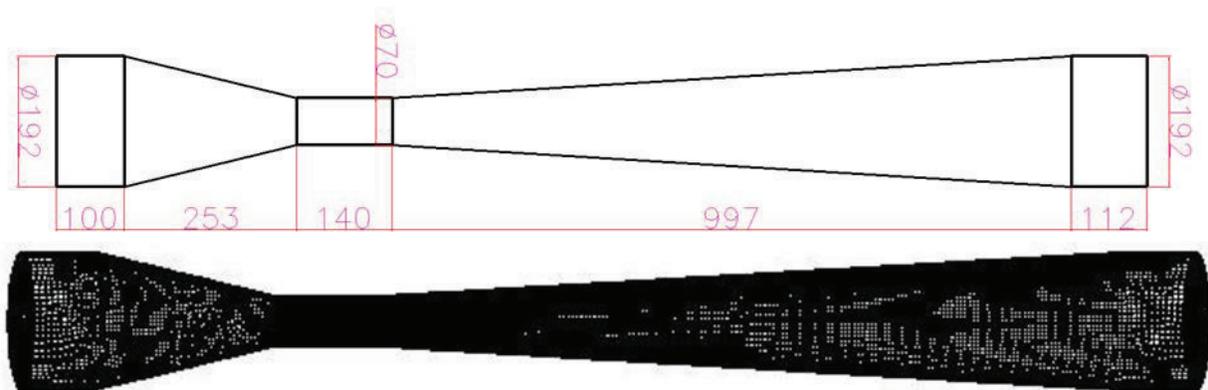


**Fig 1: Geometry and computational mesh of circular Venturi scrubber (unit:mm)**

The finite volume method was employed to obtain the numerical simulation of the dispersed three-phase flow through the venturi scrubber. Using a coupled SIMPLE algorithm, the RANS and k−ε equations were set to a simulation framework to obtain the converged gas only flow field. Standard wall function was implemented as y+ for the mesh >50. The droplets and aerosol particles were then introduced as surface injections at the orifice and the venturi inlet respectively. The dispersed particles were tracked based on the particle time step of the injection. The particle time step is defined as the time difference between two successive injections. The particle time step should be smaller than the time for collision of droplet parcels with aerosol parcels (Crowe et al. 1998). At each particle time step particles in domain are tracked and their position, velocities, diameter and injection of new particles is updated. The summary of solver settings is given in the table 1.

**Table I. Summary of solver settings**

| Solver | Air: Single phase conservation equations Droplets and aerosols: Discrete Phase Model | |
|---|---|---|
| **Viscous model** | Turbulent RNG *k-epsilon* model with standard wall function | |
| **Particle time step** | 1e-05 sec | |
| **Breakup model** | Wave model | |
| **Boundary Conditions***:* | Operating Pressure: 0.1 MPa | |
| **Region** | Type | Specification |
| **Venturi Inlet (air)** | Velocity Inlet | 9 m/s |
| **Outlet** | Pressure Outlet | Atmospheric pressure |
| **Orifice** | Injection-1 | Mass flow rate:(i) 0.296 kg/s; dia: 2.5e-03 m |
| **Venturi Inlet (aerosol)** | Injection-2 | Mass flow rate: 5e-07 kg/s; dia: 1e-06 m |

## 4. RESULTS AND DISCUSSION

The gas flow field was solved using Reynolds Averaged Navier Stokes Equation with k-ε turbulence model. Then droplets and dust were introduced through the throat orifice and the venturi inlet respectively. The numerical study was carried out using the models described in the previous section and the results were compared to experimental measurements by Haller et al. (1989). The gas flow velocity was limited to 70 m/s in the throat section while liquid loading is 1.1 l/m$^3$. Quartz was used as aerosol and its concentration was kept at 5e-07 kg/s. The inlet distribution of the aerosols was uniform and the size was fixed to 1μm.

The centre plane contours of the gas velocity are shown in Fig. 2 for the three phase flow and the gas only flow respectively. Clearly the gas velocity, due to injection, was reduced in the near axis region of the throat section. The droplets were accelerated by receiving the momentum of the gas in the orifice region of the venturi throat. Therefore, to satisfy mass conservation, the gas velocity had to have a higher velocity (near wall region of throat section) in the three phase flow compared to the gas only flow. The accelerated droplets achieve their maximum velocities within the throat, as is observed in Fig. 3. The plot shows the variation of axial velocity of the liquid droplets as it moves along the scrubber length. The stokes number for aerosol particles, calculated from these flow conditions, is much greater than 1; this specifies that the particle remains unaffected by the fluid velocity and does not influence it. Thus, the aerosol particle collides with the droplet rather than flowing around it.
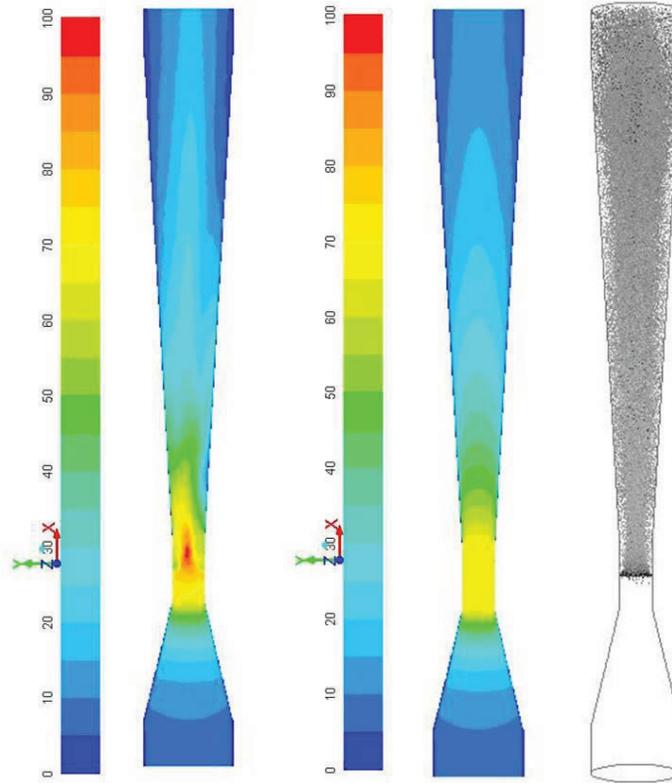
**Figure 2. Contours of (a) gas only flow velocity (b) three phase gas velocity for l/g=1.1; (c) Droplet distribution for l/g=1.1 l/m³**
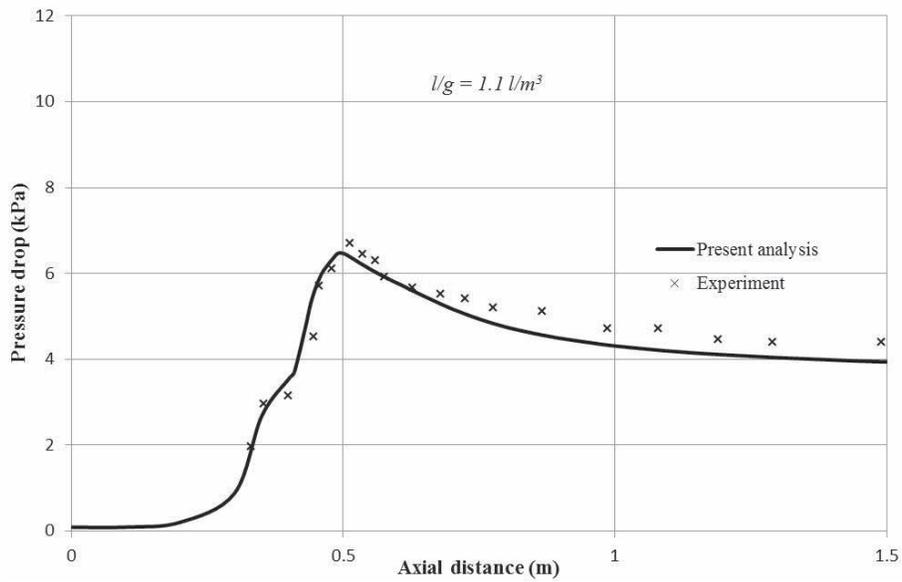


**Figure 3. Pressure drop profiles as a function of axial distance when $V_{g,th}$=70 m/s and l/g=1.1 l/m³**

The pressure drop in venturi is attributed to momentum exchange of droplets and gas, momentum drop of film, gravitational force and frictional drop (Allen et al. 1996). However, it has been reported in the literature that liquid film can be considered to be negligible in the analyses (Vishwanathan et al. 1998) so it is not considered in the present study. The pressure drop for gas throat velocity 70 m/s and liquid loading 1.1 l/m$^3$ is shown in Fig 3. As evident from Fig. 3 the pressure dropped continuously up to the converging section and stayed nearly flat to the liquid injection point of x = 0.423 m. The pressure value further decreases in the throat section which can be explained by the added resistance offered by the entrained droplets. This pressure drop helps in accelerating the droplets in the throat section. The pressure drop shows a peak at x=0.5m throat end implying the entrained droplets continue to gain momentum from gas phase which is also reflected in Fig 4. Finally the pressure in the diffuser was recovered to some extent. The overall pressure drop is lower than experimentally measured for both the cases. These discrepancies can be explained due non-inclusion of other phenomena like droplet coalescence, turbulence coupling etc.
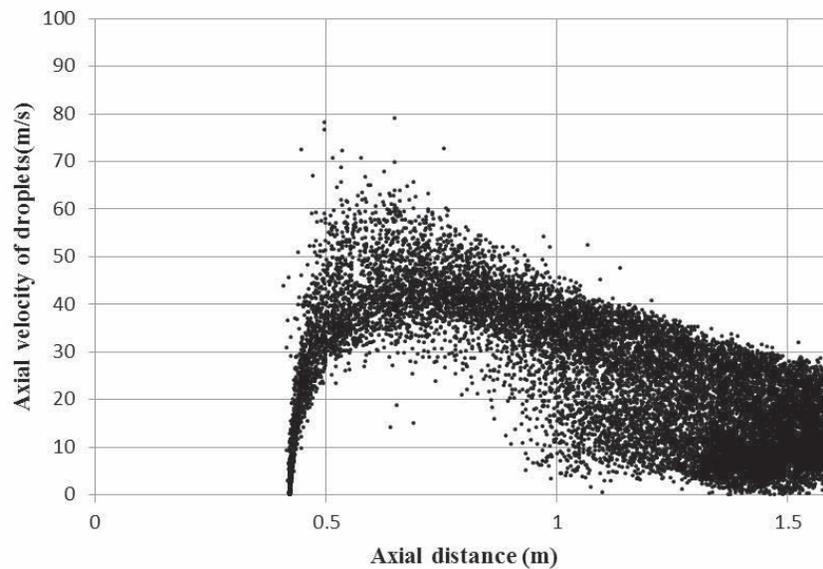


**Figure 4. Droplet axial velocity as a function of axial distance when $V_{g,th}$=70 m/s and l/g=1.1 l/m$^3$**

The droplet diameter distribution is shown at x=0.423 m (just after injection) and 0.493 m (throat end) is shown in Fig 5. Break-up of particle just after injection is observed and droplet diameters of a wide range is observed. However, at the end of throat section where the axial velocity reaches a peak the droplet diameters show uniformity in sizes with maximum concentration in the range of 150-300 µm. After x=1m the pressure drop recovers and gains a constant value suggesting that the relative velocity and the break-up post that is not significant. The droplet distributions also reflect that at the point of injection droplets are located at the periphery of domain while at the end of throat the droplets occupy centre location of the domain. Also at exit of venturi scrubber the centre-line jet velocity and the axial velocity is of the same order as concluded from centre-plane contour and axial velocity distribution plot.
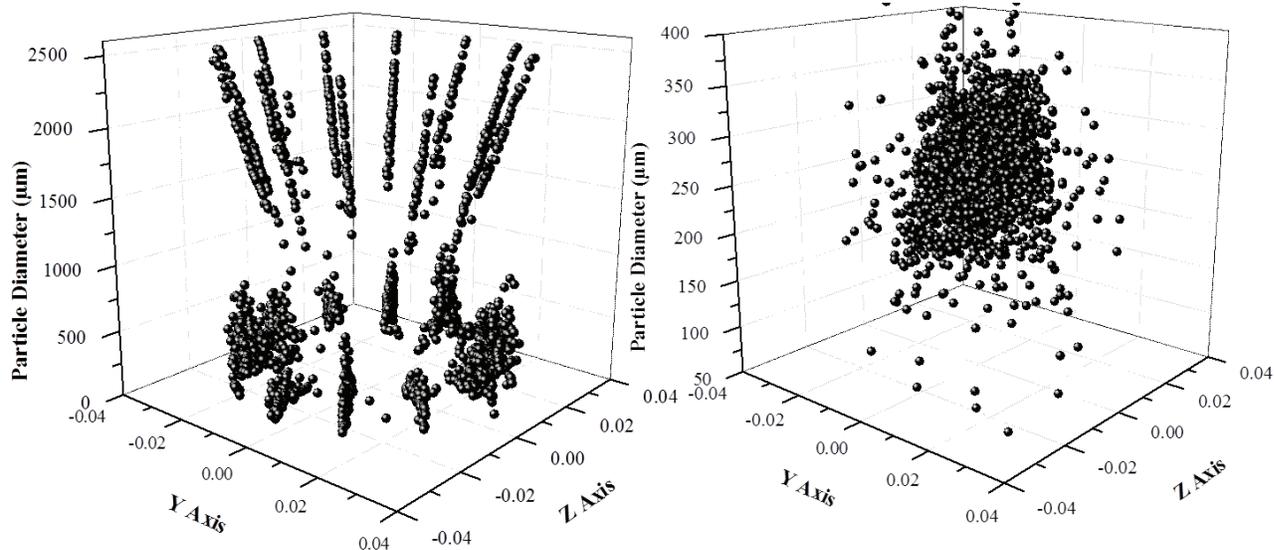
**Fig 5. Droplet diameter distribution just after injection(x=0.423) (left)
and at the throat end(x=0.493m) (right).**

The collection efficiency of the scrubber is dependent on the spatial distribution of droplets and aerosols in the computational cell. As discussed earlier in the model description single particle target efficiency is calculated for individual droplet parcels in the cell. The collection efficiency of domain is calculated by weighing it with the number of participating cells in the domain. The paper reports the analyses of collection efficiency in the throat section only. The calculated efficiency for the case where liquid is loading 1.1 l/m3 is predicted to be 87% with a target efficiency of 94%. The values reported in the literature are 98% and 95.4% respectively for collection efficiency and target efficiency. The under-predicted values may be observed due to limitation of throat section consideration and inaccurate prediction of drop sizes. The higher sized drop values have higher Stokes number and are less affected in the venturi scrubber. Also smaller droplets have larger surface area for collision, will provide uniform domain coverage for collision dynamics and have higher residence time. Therefore, an accurate prediction of droplet diameter is a necessity for a better model.

## 5. CONCLUSION

A 3-D numerical model has been proposed for the prediction of pressure drop and collection efficiency of AHWR design specific venturi scrubber. The new model solved three phase flow in venturi scrubber employing Eulerian-Lagrangian approach. The aerosols are treated as passive contaminants in the flow while water jet introduced in the nozzles induce turbulence in the flow. Atomization model for jet disintegration into droplets, droplets collision and interaction between the dispersed phases has been included in the study. Presently, validation studies carried out on published results are shown. The pressure drop and collection efficiencies in the throat section are under-predicted. This is mainly due to a) inaccurate prediction of droplet diameter, b) not including liquid film model and c) only analyzing throat section.

NOMENCLATURE

| | | | | |
|---|---|---|---|---|
| $C_D$ | drag coefficient of particle (dimensionless) | | $N_s$ | number of particles in one aerosol parcel |
| $K_p$ | inertial impaction parameter (dimensionless) | | $N_d$ | number of particles in one droplet parcel |
| $d_p$ | droplet diameter (m) | | $\tau$ | particle relaxation time (sec) |
| $d_s$ | aerosol diameter (m) | | $dV$ | volume of computational cell (m$^3$) |
| $N_{cap}$ | number of aerosol particles captured by one droplet in a computational cell | | $N_{cell}$ | total number of aerosol particles captured by all droplets in a computational cell |
| $u_d$ | velocity of droplet (m/s) | | $V_{g,th}$ | gas throat velocity (m/s) |
| $\mu_g$ | viscosity of gas (Pa s) | | $z$ | distance from venturi inlet (m) |
| $\eta$ | target efficiency (dimensionless) | | $l/g$ | liquid to gas volumetric flow rate ratio (l/m$^3$) |
| $u_s$ | velocity of aerosol (m/s) | | $Re$ | Reynolds number for particle (dimensionless) |
| $C_{D,sphere}$ | drag coefficient of sphere (dimensionless) | | $t_{cb}$ | Column fracture time of liquid jet (sec) |

**REFERENCES**

1. A. Majid, Y. Changqi, S. Zhongning, W. Jianjun, G. Haifeng, CFD simulation of dust particle removal efficiency of a venturi scrubber in CFX, Nuclear Engineering and Design, 256, 169– 177, 2013.
2. A. Sharifi, A. Mohebbi, A combined CFD modeling with population balance equation to predict pressure drop in venturi scrubbers, Res Chem. Intermed., 40, 1021–1042, 2014.
3. C. Crowe, M. Sommerfeld, Y. Tsuji, Multiphase Flows with Droplets and Particles, CRC Press LLC, 1998.
4. C. Goniva, Z. Tukovic, C. Feilmayr, T. Burgler, S. Pirker, Simulation of off gas scrubbing by a combined Eulerian-lagrangian model, Seventh International Conference on CFD in the Minerals and Process Industries, 2009.
5. F. Mayinger, M. Neumann, Dust collection in Venturi-Scrubbers, Ger. Chem. Engg., 1, 289-293, 1978.
6. H. Haller, E. Muschelknautz, T. Schultz, Venturi Scrubber Calculation and Optimization, Chem. Eng. Technol. 12, 188-195, 1989.
7. R. H. Boll, Particle Collection and Pressure Drop in Venturi Scrubbers, Ind. Eng. Chem. Fundam., Vol. 12, No. 1, 1973.
8. R.W.K Allen, A. Santen, Designing for pressure drop in Venturi scrubbers: the importance of dry pressure drop, The Chemical Engineering Journal, 61, 203-211, 1996.
9. S.A. Morsi, A.J. Alexander, An investigation of particle trajectories in two phase flow systems, J. Fluid Mech., 55(2), 193-208, 1972.
10. S. Calvert, Venturi and Other Atomizing Scrubbers Efficiency and Pressure Drop, AIChE Journal, 392-396, 1970.
11. S.I Pak, K.S. Chang, Performance estimation of a Venturi scrubber using a computational model for capturing dust particles with liquid spray, Journal of Hazardous Materials B, 138, 560–573, 2006.
12. S. Viswanathan, Examination of liquid film characteristics in the prediction of pressure drop in a venturi scrubber. Chem. Eng. Sci. 53, 3161–3175, 1998.
13. V.G. Guerra, R Bettega, J.A.S. Gonçalves, and J.R. Coury, Pressure Drop and Liquid Distribution in a Venturi Scrubber: Experimental Data and CFD Simulation. Ind. Eng. Chem. Res. 51, 8049−8060, 2012.
14. F. Ahmadvand, M.R. Talaie, CFD modeling of droplet dispersion in a Venturi scrubber. Chemical Engineering Journal 160,423–431, 2010.
15. P.K. Wu, K.A. Kirkendall, R.P. Fuller, Breakup processes of liquid jets in subsonic crossflows. Journal of Propulsion and Power,13,No.1,64-73,1997.